Title:

A systematic screen of breast cancer patients' exomes for retrotransposon insertions reveals disease associated genes

Authors:

Sylvia De Brakeleer, Jacques De Grève and Erik Teugels*

Affiliation:

Laboratory of Molecular and Medical Oncology

Vrije Universiteit Brussel

Laarbeeklaan 103, 1090 Brussels

Belgium

Email adresses:

Sylvia De Brakeleer sylvia.debrakeleer@gmail.com

Jacques De Grève Jacques.DeGreve@uzbrussel.be

Erik Teugels eteugels@vub.be

*corresponding author

ABSTRACT

Background: Retrotransposons are genetic elements that jump within the genome via an RNA intermediate. Although they had a strong impact on human genome evolution, only a very tiny fraction of them can be reactivated nowadays, most often with neutral or detrimental consequences. The pathological outcomes associated with such genetic alterations are poorly investigated in the clinic, merely due to their difficult detection.

Results: We developed a strategy to detect rare retrotransposon mediated insertions in Whole Exome Sequencing data from 65 familial breast cancer patients. When restricting our search to high confidence retrotransposition events occurring in less than 10% of the samples, we identified only ten different Alu elements, two L1 elements, one SVA and two processed pseudogenes. Only two of these insertions occurred within protein coding sequences and interestingly, several of the targeted genes have been previously linked to cancer, in three cases even to increased breast cancer risk (*GHR*, *DMBT1* and *NEK10*). When investigating the molecular consequences of four Alu insertions at the mRNA level, we found that the element present in the 3'UTR of *GHR* repressed expression of the corresponding allele. Moreover, the analysis of a near exonic Alu insertion in *PTPN14* (a mediator of *P53* tumor suppressor activity) revealed that this gene was imprinted and that the presence of an intronic Alu element can lead to loss of imprinting.

Conclusions: Our data underline the relevance of incorporating the search for uncommon retrotransposition events in Next Generation Sequencing pipelines when analyzing patients with a suspected genetic disease.

KEYWORDS: retrotransposition, Alu, L1, pseudogene, breast cancer predisposition, exome, *GHR*, *PTPN14, ZNF442, C1orf194*

BACKGROUND

More than 50% of the human genome is built up with sequences that originated from the activity of transposable elements[1], mainly retrotransposons which are able to move to new locations in the genome via an RNA intermediate using the copy/paste principle[2-4]. L1 retrotransposons belong to the LINE (long interspersed element) superfamily and are the only transposons still active in human. Full length L1 elements (~6kb long) code for the proteins necessary for retrotransposition, including a reverse transcriptase. Although L1 sequences represent about 17% of the human genome, only a very small fraction of them (80-100 copies) retained their transposition capacity[5, 6]. Alu and SVA retrotransposons (about 300 and 1400bp long respectively) are SINEs (short interspersed elements) and do not code for proteins. Rather, they are fully dependent on L1 retrotransposition and parasitize its propagation system. Accidentally, cellular RNA can also misuse the L1 retrotransposition machinery resulting in the generation of processed pseudogenes[7]. The CpG rich sequences present in L1 promoters, Alu and SVA elements are sites for DNA methylation and heterochromatin formation, causing epigenetic silencing[8]. Interestingly, the vast majority of evolutionary stabilized Alu insertions are located in gene-rich regions. They are often embedded in sequences encoding pre-mRNAs or mature mRNAs, usually as part of their introns or UTRs were they can potentially contribute to transcriptome variation[9].

In 1985 the first de novo Alu element insertion was reported in a B cell lymphoma[10]. Three years later, Kazazian et al.[11] reported a Haemophilia A causing L1 element insertion in germline DNA. In a review article published in 2016[6], the list of retrotransposons associated with human diseases counts 124 entries. Obviously, the number of disease causing retrotransposition events identified in human[12] is increasing steadily, but the attention these mutations receive in the clinic is still very poor when compared to classical mutational events (nucleotide substitutions and small insertions/deletions). When searching for breast cancer (BC) predisposing mutations in high risk families, we previously identified one Alu insertion in exon 11 of *BRCA1* and one Alu insertion in exon 3 of the *BRCA2* gene[13], this last one appeared later on to be a recurrent founder mutation restricted to the Portuguese population[14]. When Next Generation Sequencing tools were introduced in the diagnostic field, only few labs adapted their IN SILICO pipeline to allow the identification of pathogenic retrotransposition events in the genes they analyze[15, 16]. In the present work, we developed a strategy allowing the detection of uncommon retrotransposition events in Whole Exome Sequencing (WES) data using BAM files generated from a cohort of familial breast cancer patients previously used to identify more classical cancer predisposing mutations[17]. In a second step, we investigated the molecular consequences generated by 5 candidate pathogenic Alu insertions revealed during our screen, and highlight the relevance of screening for rare retrotransposition events in the clinical context.

RESULTS

IN SILICO screen for retrotransposition mediated insertions

Because of their shared mechanisms of transposition using an RNA molecule as intermediate, retrotransposons all bear a long polyA tail at their 3' extremity. Also, their specific mechanism for insertion into the target DNA results in the duplication of a short sequence at the position where the retrotransposon has integrated. This duplicated sequence (called Target Site Duplication or TSD) is usually between 4 and 20 nucleotides long and flanks the retrotransposon specific sequences. We exploited those two characteristics to identify retrotransposon insertions not present in the human reference genome (hg19) using WES data generated with the SeqCap EZ Exome v3.0 kit from Roche. Paired-end sequencing usually generates read pairs that perfectly map in close proximity on a reference genome. However, the presence of a non-reference retrotransposon insertion will result in read pairs that do not map closely (Figure1). We selected these discordantly mapped read pairs by applying the open-source RetroSeq software[18] on the BAM files previously obtained from 65 BC patients[17] (positive *BRCA1* control included), with a first additional restriction that one read of the discordantly mapped read pairs must harbor a long polyA stretch. On average, we obtained 987 candidate insertions for each patient. When introducing additional filtering steps (using an Excel program) to remove false positives and frequently occurring non reference polymorphic insertions, we ended with a list counting only 32 different candidate polyA containing insertion sites for the pooled 65 patients (Additional file 1). A detailed description of our detection strategy and its application on a positive control sample is presented in the Method section, wherein we also compare two widely used exome enrichment kits.

High confident retrotransposition mediated insertions

When performing a manual selection (using the Integrative Genomics Viewer: IGV[19]) for the presence of a TSD on the 32 polyA containing insertions we had identified, we ended up with 18 high confidence candidates retrotransposon insertions (Table 1). The further characterization of these retrotransposition mediated insertions (12 Alu, 2 L1, 1 SVA and 3 pseudogenes, see Table 1) was made possible by the presence of a stretch of nucleotides (maximum ~50bp long) in a fraction of the aligned read pairs that do not match with the reference sequence, but corresponded the 5' extremity of the inserted sequence. These sequences could be identified using available web tools (see Methods). A representative screenshot showing the outcome of an IGV analysis of the genomic region wherein the Alu element integrated into the BRCA1 gene of our positive control sample is presented in Figure 2. Only 2 out of the 18 retrotransposon mediated events occurred within protein coding regions (Alu element in *ZNF442* and *UQCR10* transcript in *C1orf194*, see Table 1) which might be surprising since WES probes are expected to be specifically designed towards exonic sequences. Indeed, according to the kit provider (Roche) only protein coding parts of the transcripts are targeted, but for exons that are smaller than 100 bp, the target region is extended to 100 bp. Nevertheless, we expect that the large majority of retrotransposition mediated insertions occurring in the well covered protein coding regions will be picked up with our screen, their low incidence being in agreement with the literature[5, 20, 21]. Conversely, we are convinced that a significant fraction of the polymorphic retrotransposons located in the vicinity of protein coding regions (regions often poorly or not covered at all by WES) is missed with our WES based approach, although the large majority of identified insertions (15/17, positive control excluded) are located in intronic, 3'UTR, promoter or even intergenic sequences. As a sufficient coverage at sequencing is essential to allow the identification of polymorphic retrotransposons in the non-coding regions, we wanted to estimate

the number of false negative carriers of such highly confident retrotransposition mediated insertions among the 65 samples we investigated. Therefore, all samples were rescreened for the presence of the 18 IN SILICO identified insertion types using IGV (see Table 1). All insertions identified with the IN SILICO pipeline could be confirmed with IGV analysis (no false positives). As expected, IGV inspection revealed higher rates of carriers for 9 insertions (Table 1). In two cases, insertion carriership was even observed in 50% of the samples, with IGV and IN SILICO data discrepancies being well explainable by the low coverage at sequencing. Of note, about half of the high confident retrotransposon insertions we identified are reported in the database of retrotransposon insertion polymorphisms in human (dbRIP, see Table 1).

Retrotransposon insertions in non-coding regions can affect allelic expression

To investigate the potential consequences of Alu insertions located in non-coding gene regions at the molecular level[22], we collected blood samples from available carriers (and non-carriers for control) and extracted the corresponding RNA material. Since allele specific expression levels can be monitored by Sanger sequencing only when the Alu carrier is also heterozygous for a coding SNP in the same gene, the number of suitable insAlu carriers among the 65 investigated patients was not always sufficient and additional familial BC patients were genotyped using mutation specific hemi-nested PCRs (Table 2). Sufficient blood samples could be collected to initiate the analysis of 5 Alu targeted genes (*GHR*, *GSTA5*, *NEK10, PTPN14* and *UPF2*). Sequence analyses of the cDNA regions flanking the allele discriminating SNPs revealed that the intronic Alu insertions in *UPF2* and *NEK10* do not result in an obvious decrease or increase of the mRNA levels generated from the retrotransposon targeted allele (Figure 3). In sharp contrast, the Alu insertion in the 3'UTR of *GHR* clearly resulted in allele silencing (Figure 4A) suggesting

that this Alu sequence may contain sites for microRNA directed degradation, a mechanism previously proposed to explain the occurrence of evolutionary stabilized Alu derived microRNA binding sites in the 3'UTRs of specific gene[23]. Conversely, the two available carriers of the intronic Alu insertion in *PTPN14* seem to express both alleles equally well but among the three non-carriers, one expresses virtually only one allele while the two others show a reduced expression of this same allele (Figure 4B). Partial or near absolute mono-allelic expression of *PTPN14* is in agreement with a study listing this gene as a high-confidence imprinted human gene candidate with maternal expression[24]. On the other hand, the apparent loss of imprinting (LOI) observed in the Alu carriers suggests that the integration of one single Alu element into the gene sequence of the imprinted allele would be sufficient to fully reactivate this allele, which matches with earlier observations reporting a sharp inflection in SINE content at transitions from imprinted to non-imprinted genomic regions[25]. Unfortunately, differential expression of the *GSTA5* Alu containing allele (insertion occurred in the promoter region) could not be investigated due to the very low expression level of *GSTA5* in leucocytes compared to *GSTA1* and *GSTA2* (see GeneCards.org), three homologues that are hard to discriminate when using PCR based assays (only GSTA1 and/or GSTA2 sequences could be detected after Sanger sequencing even by using gene discriminating primers for PCR, results not shown).

PolyA containing insertions without identifiable TSD

In addition to the 18 high confident retrotransposition mediated insertions for which we could identify a TSD (described above), our IN SILICO pipeline also identified 14 candidate insertion sites for which a TSD could not be deduced using IGV (see Additional file 1 and Table 3). A summary of each of the targeted gene's function is presented in Additional file 2 (see also Table

4 for PubMed hits). A lower coverage at sequencing most probably explains the problematic discovery and characterization of these polyA containing insertions. However, for eight of them we found parts of retrotransposon sequences (7x Alu, 1x L1) by analyzing the mates of the discordantly mapped mate pairs (Table 3). In addition, 7 out of these 14 expected retrotransposition events map at the same genomic position as do elements reported in the database for Retrotransposition Insertion Polymorphisms in Humans (dbRIP[26]). Consequently 10 out of the 14 polyA containing insertions can be linked to a retrotransposon, making them still strong candidate retrotransposon insertion sites with potential pathological consequences (Table 3). The high rate of confirmed retrotransposon mediated insertions observed among the candidate polyA containing insertions we identified (28 out of 32) is a good indicator for the high specificity of the followed screening strategy.

DISCUSSION

De novo retrotransposition events occurring within protein coding regions are expected to be very rare as they would strongly affect protein integrity, most often in a detrimental manner [5, 20, 21]. Our results fully match with these earlier observations as the only rare polymorphic retrotransposon that inserted exome wide into a coding sequence among our 65 patients (positive BRCA1 control excluded) was an Alu element into the *ZNF442* gene (a short summary of the function of all genes targeted with a high confident retransposon mediated insertion is presented in Additional file 3). A mutation specific PCR screen (see Table 2) detected this variant in only one out of 710 familial BC patients. Since this patient has North African roots, we cannot

exclude that the mutation is more prevalent in that region. *ZNF442* has been poorly investigated till now (see outcomes of PubMed searches for the different targeted genes in Table 5) although the gene has been reported as a good candidate driver gene for the neoplastic process of breast and colorectal cancer[27]. The second identified retrotransposition mediated event that destroys protein integrity is the UQCR10 transcript inserting into the *C1orf194* coding sequence (creating a *UQCR10* processed pseudogene). This polymorphic insertion has been previously observed[7, 28] and was present in 7 of our 65 samples. The mutant allele is unable to produce normal C1orf194 protein, but we cannot exclude that the *UQCR10* pseudogene is expressed as a recombinant mRNA leading to overproduction of UQCR10 protein since a near full length UQCR10 transcript (from c.-15 till polyA tail) inserted in the 5' coding region (c.58_70) of the *C1orf194* gene in the same orientation (Table 1). Little is known about these two genes, but none has been linked to breast cancer yet. Interestingly, two seemingly dominant heterozygous missense mutations in *C1orf194* were recently associated with Charcot-Marie-Tooth disease[29], the most common form of inherited peripheral neuropathy. The authors reported a Ca^{2+} regulatory function for C1orf194 and therefore suggested that this gene (and consequently any mutated form at it) may also be associated with other neurodegenerative disorders characterized by altered Ca^{2+} homeostasis.

The large majority of high confident retrotransposon insertions we could identify were located in non-coding regions (15 out of 17). However, such regions are not the primary targets when performing WES and consequently their coverage at sequencing will often be (very) low, or they will not be covered at all. Therefore, we believe much more intronic (near exonic) and UTR located polymorphic retrotransposons escaped our attention, the 15 ones reported herein

representing the tip of an iceberg. The majority of the identified retrotransposon insertions incorporated into intronic sequences, close to the intron-exon boundaries. The genes targeted by these retrotransposition events can be linked to several biochemical processes (Additional file 3) that might be involved in breast cancer development: they can have a tyrosine kinase activity (*NEK10*[30, 31]), a Tyrosine phosphatase activity (*PTPN14*[32]), being involved in the ubiquitination process (*UBA6*[33]), in the posttranscriptional methylation of internal adenosine residues in eukaryotic mRNAs (*METTL3*[34, 35]), in the regulation of the nonsense mediated decay pathway (*UPF2*[36]), have a suppressive role in osteosarcoma progression (*TMIGD3*[37]) or are considered as candidate tumor suppressor gene for different cancer types (*DMBT1*[38-40]). Interestingly, four of the five intronic Alu insertions occurred in antisense orientation, suggesting that these insertions might contribute to the generation of alternative transcript forms[41]. We also identified two retrotransposon insertions in 3'UTR gene regions (in *GHR* and *HSD17B12*), one in the promoter of *GSTA5* (a glutathione S transferase catalyzing the conjugation of reduced form of glutathione to xenobiotic substances for the purpose of detoxification) and three in intergenic regions (in one case with nearest gene linked to BC: *MIF-AS1*[42]). More convincing for their role in breast cancer predisposition is that 3 retrotransposons inserted into a gene that had been previously associated to breast cancer risk (*GHR*[43-45], *DMBT1*[46-48] and *NEK10*[49, 50]*).* The potential cancer risk associated to these particular mutations should be confirmed by investigating a much higher number of BC cases and controls.

Furthermore, we could successfully investigate the consequences of four different Alu element insertions in non-coding gene regions at the molecular level by determining the relative expression level of the wild type versus mutant allele in leucocytes. Analysis of the Alu insertions in NEK10 and UPF2 did not reveal a marked decrease or increase of the mRNA levels

generated from the retrotransposon targeted alleles. Nevertheless, a pathogenic (or protective) contribution by these mutated alleles cannot be excluded yet, as they may for instance generate splicing alterations that cannot be detected with the performed test or may result in cell type specific effects not observed in leucocytes. Moreover, the recently revealed mechanism of onco-exaptation[51, 52] whereby cryptic regulatory elements within transposons can be epigenetically reactivated in precancerous cells may also drive cancer risk. In sharp contrast, the Alu insertion in the 3'UTR of *GHR* clearly resulted in allele silencing**.** Since several association studies indicated that *GHR* is implicated in breast cancer predisposition[43-45], it is tempting to designate the Alu insertion in *GHR* as (one of) the causal mutation(s) for the reported cancer risk modulation. The interpretation of the data obtained when investigating the Alu insertion in *PTPN14* was more challenging since (near) mono allelic expression was already observed in the three patients that did not carry the germline Alu insertion in PTPN14. Fortunately, literature digging revealed a table wherein PTPN14 was listed as a high-confidence imprinted human gene candidate with maternal expression[24]. The LOI observed in our two Alu carriers suggests that the integration of one single Alu element into the imprinted PTPN14 gene allele would be sufficient to fully reactivate this allele[25]. The observed LOI also suggest that both patients inherited the mutated PTPN14 allele from their father (could not be verified) and that in case the mutated allele is maternally inherited, LOI will not be observed. Since *PTPN14* was recently identified as a mediator of the tumor suppressor activity of *p53* and regularly mutated in cancer[32], its imprinted nature and the loss of imprinting (LOI) induced by particular mutations are two elements that contribute additional levels of complexity to the molecular mechanism leading to cancer when the *PTPN14* gene is involved.

CONCLUSIONS

Our study indicates that raw WES data obtained from clinical samples (whose availability is exponentially growing) hide a manageable number of retrotransposition mediated polymorphic mutations that can be dug up when using appropriate IN SILICO tools. A significant fraction of these mutations will affect gene function, even when located outside protein coding regions, and consequently may be (one of) the pathogenic factor(s) responsible for a patient's disease. Our investigation was restricted to 65 non BRCA1/2 familial BC patients, but much more patients should be analyzed (in future genome wide) to obtain a broader view of all possible retrotransposon mediated insertions involved in the disease, and to determine their respective molecular and pathogenic consequences. Moreover, transposon mediated insertions resulting in modified breast cancer risk may also generate other clinical phenotypes. For example, the growth hormone receptor (which is encoded by the *GHR* gene) is expressed in a broad range of tissues and involved in fundamental biological processes such as growth promotion, metabolism, cell division and regeneration[53], the most typical clinical syndrome associated to GHR deficiency being dwarfism (Laron syndrome). Accordingly, the clinical consequences associated to the presence of an Alu insertion in the 3'UTR of *GHR* (which leads to allele silencing) are most probably not limited to breast cancer risk. As pathogenic retrotransposon insertions are not limited to the familial BC syndrome, the described mutation screen (or an alternative version of it, e.g. for the analysis of WES data obtained with the exome capture kit from Agilent) should be applied for all diseases with a suspected genetic etiology. Indeed, screening patients with a specific genetic disease will enrich for insertions in genes involved in that disease (in preparation). Centralized databases registering all identified polymorphic retrotransposition events should be further expanded[7, 26, 54], with inclusion of population specific allele

299 frequencies, as is the case for classical variations. In order to identify good candidate pathogenic
300 Alu element insertions, Payer et al.[55] used the outputs of GWAS studies to restrict their search
301 to genomic loci previously implicated in disease risk. Conversely, our data indicate that
302 microchips should be developed allowing genome wide genotyping for the presence of this
303 particular type of polymorphic insertions, in order to perform retrotransposition specific
304 GWAS's for a multitude of diseases or traits. Finally, the genome wide identification and
305 investigation of polymorphic retrotransposon insertions in clinical samples will not only lead to a
306 better understanding of diseases, but will also contribute to elucidate more basic genetic
307 mechanisms such as gene imprinting, and will help to evaluate the impact that de novo
308 retrotransposition mediated insertions still have on human genome evolution.

309

310

311 **METHODS**

312

313 **Patient Material**

314 A WES study using the SeqCap EZ Exome v3.0 kit from Roche has previously been performed
315 using blood samples from probands of 65 unrelated high risk BC families with the aim to
316 identify classical cancer predisposing mutations (protein truncating SNPs and Indels, and splice
317 site mutations)[17]. All patients were recruited at the UZ-Brussel hospital and met the
318 requirements for a diagnostic *BRCA1* and *BRCA2* mutation analysis. All except one (the positive
319 control: c.1739_1740insAlu in *BRCA1*[13]) were negative for a pathogenic *BRCA1* or *BRCA2*
320 mutation. A large subset of these 65 patients (57) belongs to families with at least two first

321 degree blood relatives with BC. The FastQ files generated during this previous study were reused
322 for the present study. The genomic DNA from the positive control was resubmitted for WES
323 analysis using the SureSelect Human All Exon V6 kit from Agilent (performed by BGI
324 Genomics Co, China) to compare both WES approaches. In addition, blood samples obtained
325 from 710 probands from independent non BRCA1/2 BC families (including the 65 probands
326 used for the WES analysis) were used for a PCR based genomic screen to identify additional
327 carriers of Alu element insertions in case insufficient samples were available for RNA analysis.

328

329 **Strategy for retrotransposon detection using WES-BAM files**

330 Binary alignment files (BAM files) are outputs (binary versions) of a short read aligner (e.g.
331 BWA[56]) that can map the read pairs generated during the sequencing process (paired-end
332 sequencing) towards a reference sequence, for instance the reference human genome (hg19). In
333 particular circumstances, these read pairs are discordantly mapped while generated from the
334 same small genomic fragment, meaning that the mate reads map at very different positions on the
335 reference genome.

336 To trace retrotransposon insertions not present in the human reference sequence we used, in a
337 first try-out, the open-source RetroSeq software described by Keane et al.[18] as this software
338 can be run on virtually any computer[57]. This software needs as input a BAM file (we used the
339 WES BAM file generated with a positive control sample harboring the c.1739_1740insAlu
340 mutation in *BRCA1*; the library was prepared using the exome capture kit SeqCap EZ Exome
341 v3.0 from Roche), a reference genome (hg19) and a library of mobile element sequences.
342 RetroSeq operates in two phases, the first being the discovery phase where discordantly mapped
343 (and one end mapped) mate pairs are screened for the presence of a mobile element and in the

affirmative assigned to a particular type of mobile element. In the second phase (calling phase), the sequence of the anchoring mate read is used to localize the polymorphic mobile element on the reference genome. Unfortunately, when applying RetroSeq on our positive control sample we could not detect the Alu insertion in *BRCA1*. RetroSeq is primarily designed to identify non reference mobile elements in Whole Genome Sequencing data, while companies that design kits for exome enrichment try to avoid the capture of nucleotide fragment harboring repetitive sequences. To circumvent this obstacle, we decide in a first step to search not for mobile elements but for polyA stretches (settings: minimum 80 nucleotides long; 90% ID) within the discordantly mapped reads of each patient data set using the first module of the RetroSeq software (discovery phase). Among the discordantly mapped read pairs traceable in BAM files we expect to find those generated from genomic DNA fragments that contain both non reference retrotransposon sequences and exon (flanking) sequences (see Figure 1). By selecting discordantly mapped reads containing a long polyA stretch in one of the paired reads, we will only retain the junctions at the 3' end of the retrotransposon. The location of the mate of each polyA containing read identified during the discovery phase is recorded in a BED file by the RetroSeq program (together with additional information). This file can be recovered as a .tab file for further analysis (see Additional file 4 for the .tab file generated with the positive control sample saved in Excel).

If coverage is sufficient, several anchor reads (the mates of the polyA containing reads) are expected to align in the same genomic region. Clusters of such reads are subsequently generated when they occur within a 300 bp long genomic interval and a maximum inter read distance of 200 bp. In a next step, each cluster is represented by the anchor read expected to be closest to the integration site (TSD in case of retrotransposons) while the number of reads within each cluster

is recorded in a separate column (duplicate reads are removed). To perform these cluster calculation steps, the patient specific .tab file generated by RetroSeq is saved in Excel format, non-relevant information is first deleted and the remaining data are pasted in the first sheet of a preformatted Excel file (provided as Additional file 5). The detailed procedure for cluster calculation is described in next section. We considered clusters with three or more anchor reads as potential candidate insertion sites and retained them for further investigation. When applying this detection strategy to our 65 BC patients, we obtained on average 987 such clusters for each individual. The positive control sample (see Additional file 6) shows 641 clusters with three or more units, with a clear cluster of 17 units at the level of the Alu insertion site in *BRCA1* (TSD is at chr17:41245809-41245825).

To identify and in a second step discard the clusters (genomic regions) picked up in a large fraction of individuals (e.g. false positives resulting from technical artefacts, or highly recurrent polymorphic insertions not present in the reference genome), the Excel outputs obtained from each BC patient were pooled (keeping patient ID tracked) and clusters were again generated. Candidate genomic insertion sites detected in more than 10% of the samples (corresponding to clusters with more than 6 units for the BC cohort) were identified and subtracted from the patient specific output data. After this filtering step, on average 9 clusters with 5 or more reads are obtained for each individual. Visual inspection using the IGV software revealed that the majority of the remaining candidate insertion sites are generated by the presence of a polyA stretch in the reference sequence that resulted in DNA polymerase slippage during the NGS process. Consequently, these candidate genomic insertion sites were manually tracked and listed, and used for subsequent filtering. Additional file 7 provides a preformatted Excel file to perform the combined filtering steps. After filtering, only half of the BC patient samples presented a

candidate insertion event (31/65). One patient presented 4 such events (Additional file 1). To minimalize the possibility that these candidate insertion sites would be missed in a subset of individuals because of poorer coverage, all genomic positions identified as insertional target sites during the first screening round in any individual (positions deduced from the presence of a cluster with minimum 5 anchor reads) were re-screened for the presence of a smaller cluster (3 or 4 reads) in all individuals (Additional file 1, columns M & N). Further IGV inspection allowed the identification of a TSD in a significant fraction (18/32) of the obtained candidate insertion sites, strongly suggesting that a retrotransposition event had occurred at those genomic locations (Additional file 1, column K). For validation purposes, the presence or absence of each of these 18 insertions was verified in each of the 65 patients using IGV (Table 1). The recovery rates obtained IN SILICO and manually using IGV matched very well except for two insertions (the *SET* transcript in *DPP10* and an Alu element in *HSD17B12*), the discrepancies being explainable by the poor coverage at sequencing. For the identification of the inserted sequences, we used the Dfam database of repetitive DNA families[58] (https://dfam.org/home) and the Basic Local Alignment Search Tool (https://blast.ncbi.nlm.nih.gov/Blast.cgi) (Additional file 1, column I). As only small stretches of nucleotides (about 50 bp long) from the 5' end of the inserted sequences can be deduced from the WES generated data, it was not possible to further define the sub-family of the identified retrotransposons.

A screenshot showing read visualization by IGV of the region were the Alu insertion occurred in the positive control sample (*BRCA1*) when using the SeqCap EZ Exome v3.0 kit from Roche for exome capture is presented in Figure 2. A corresponding screenshot showing read visualization when using the SureSelect Human All Exon V6 kit from Agilent is presented in Figure 5. Note that very few discordantly mapped reads are observed when using the Agilent kit, indicating that

413 the detection strategy we described here above is unable to detect retrotransposon insertions
414 when using the WES BAM files generated with this kit, although several other identifiers of an
415 Alu insertion are clearly present and useable for the development of an adapted IN SILICO
416 pipeline.

417

418 **Procedure for cluster calculation starting with the data obtained from RetroSeq:**

419 Save the RetroSeq generated tab. file in Excel format and delete the 2 last columns (the .tab file
420 generated with the positive control sample is provided as "Additional file 4").

421 Remove all lines not referring to an autosome or to chX (all samples are from females).

422 Sort (A>Z) according to sign in last (6^{th}) column.

423 Select/copy all filled cells and paste in Sheet 1 ("calculate cluster") of the preformatted Excel file
424 for cluster calculation (Additional file 5).

425 In this Sheet 1, select for "TRUE" in column I (OR) and select/copy all filled cells in columns A
426 to J.

427 Paste the data in Sheet 2 ("simplify cluster"), and in column A, order by "color". Delete the
428 entire rows corresponding to the cells with pink background (this will remove duplicates).

429 In column O (chr), deselect "blank" and select/copy all informative cells in columns O to U.

430 Paste these data in Sheet 3 ("all clusters"), and deselect "2" in column G (to keep clusters with
431 minimum 3 reads).

Select/copy all filled cells and paste in Sheet 4 (annotation list, use the first column for sample ID). The positive control sample will generate 641 clusters (see Additional file 6).

Procedure to filter out the clusters of secondary interest (false positives or clusters highly recurrent among patients):

Based on the data we obtained from our 65 samples, we generated a table (first sheet of Additional file 7) listing (a) all clusters with minimal 3 reads that were observed in 6 or more of our patients (= clusters present ~10% or more of the samples) and (b) all clusters that resulted from the presence of a polyA stretch in the reference sequence. This table was subsequently used to identify and discard the less relevant clusters from the patient specific cluster lists (as described above). This list is provided with the only intension to familiarize with the described procedure. The content of this list can depend on the type and number of samples used for its generation (type of disease, ethnicity…) but also on the followed wet and dry bench procedures.

Select/copy all filled cells of Sheet 4 (annotation list) obtained from a patient specific cluster calculation (see above).

Open Sheet 1 (comm65>=6 + sample) of the preformatted Excel file for cluster filtering (Additional file 7) and paste the data (in column A) down the preexisting list.

Apply Sort (A>Z) on column C (start) and thereafter on column B (chr).

Select/copy the generated dataset and paste in Sheet 2 (calculate cluster_com65>=6).

Select for "0" in column L ("cluster"), for "FALSE" in column K ("OR") and for "sampleID" in column A.

Select/copy/paste clusters with five or more reads to the "results" Sheet 3.

The obtained candidate insertion sites (represented by each of the generated clusters in Sheet 3) can be manually validated by IGV inspection of the corresponding BAM files at the indicated positions.

Hemi-nested PCR's for genomic validation and screen

All uncommon Alu element insertions identified with high confidence (presence of a TSD) within or close to exonic gene sequences or promoter sequences (7 in total, see Table 1) were validated by a 2 step PCR. During the first step, and starting with an input of 6.25 ng genomic DNA, primers flanking the suspected integration site are used to generate a 200-300 bp long PCR fragment. This fragment is used as template (after 2000x dilution) for the second step of the hemi-nested PCR wherein one primer of the first step PCR is used in combination with an Alu specific primer. The first step of the nested PCR should work for all genomic DNA samples. The second step will work only when the patient is carrier of the targeted Alu insertion and the appropriate primer combination is used. Both PCR steps were run on a real-time PCR instrument (LightCycler 480 II from Roche). DNA samples from Alu carriers (and negative controls) according to our WES screen were used for validation. During the first step, an amplification with reproducible Ct and melting curve was observed with all samples while during the second step only samples with an Alu insertion gave an amplification signal (with reproducible Ct and melting curve). The obtained PCR fragments were further evaluated by agarose gel

474 electrophoresis and all showed the expected size. The primers used for PCR amplification are
475 shown in Table 6. The Alu specific primer (Alu/Rev) is located in a well conserved region and
476 points to the 5' extremity of the transposon. Consequently, this primer will never allow
477 amplification of the 3' extremity (polyA tail) of the transposon. The choice of the second primer
478 for the second step of the PCR will depend on the orientation of the Alu element compared to the
479 orientation of the targeted gene (see Table1, 2nd column). In order to identify additional carriers
480 of the Alu insertions characterized during the raw WES data screen, the same nested PCRs were
481 performed on genomic DNA from 710 familial BC patients (Table 2).

482

483 **Genotyping at polymorphic sites**

484 To investigate whether an Alu element that integrated into the non-coding regions of a gene
485 affects expression levels of the targeted allele, a polymorphic site allowing allelic discrimination
486 at the cDNA level must first be identified. This was done by IGV inspection of the BAM files
487 from patients that had revealed a polymorphic Alu insertion during our screen (Additional file 1).
488 To increase the number of samples that could be enrolled in the allele expression study, the
489 patients whose genomic DNA revealed an interesting Alu insertion upon mutation specific PCR
490 analysis were genotyped for the corresponding polymorphic site. PCR primers are presented in
491 Table 7. Heterozygosity was determined by High Resolution Melting Curve Analysis.

492

493 **RNA isolation, cDNA synthesis and RT-PCR**

494 RNA isolation was performed using the RNeasy Mini kit (Qiagen) with additional DNAse step
495 using manufacturer's protocol. cDNAs were prepared using Superscript II reverse transcriptase

(Life Sciences) using hexamer random primers and qPCR was performed using the SybrGreen Master kit (Roche) on a LightCycler 480 II. Primers are presented in Table 8.

Sequencing

Purified PCR fragments were Sanger sequenced by the VIB Genetic Service Facility, from the University of Antwerp.

DECLARATIONS

Ethics approval and consent to participate: Patient recruitment and blood sampling were performed according to the ethical procedures approved by the institutional ethics committee of the UZ Brussel. For the concerned cases, peripheral blood was collected after obtaining a written informed consent for a broad genomic analysis covering also incidental findings in genes predictive for other diseases.

Consent for publication: Not applicable

Availability of data and materials: a dataset allowing the reproduction of the outputs for a positive control is provided as “additional file”. Additional datasets are available on reasonable request

Competing interests: the authors declare that they have no competing interests

Funding: financial support from “Kom Op Tegen Kanker” is acknowledged

Authors’ contribution: SDB and ET conceived the project, designed and performed the experiments, interpreted the data and wrote the manuscript. JDG is responsible for patient recruitment and counselling. All authors reviewed and approved the manuscript.

523 Acknowledgements: not applicable

524

525 Authors' information (optional): not applicable

526

527

528

REFERENCES

1. Lander ES, Linton LM, Birren B, Nusbaum C, Zody MC, Baldwin J, Devon K, Dewar K, Doyle M, FitzHugh W, et al: **Initial sequencing and analysis of the human genome.** *Nature* 2001, **409:**860-921.
2. Jurka J: **Evolutionary impact of human Alu repetitive elements.** *Curr Opin Genet Dev* 2004, **14:**603-608.
3. Cordaux R, Batzer MA: **The impact of retrotransposons on human genome evolution.** *Nat Rev Genet* 2009, **10:**691-703.
4. Kazazian HH, Moran JV: **Mobile DNA in Health and Disease.** *N Engl J Med* 2017, **377:**361-370.
5. Rishishwar L, Wang L, Wang J, Yi SV, Lachance J, Jordan IK: **Evidence for positive selection on recent human transposable element insertions.** *Gene* 2018, **675:**69-79.
6. Hancks DC, Kazazian HH: **Roles for retrotransposon insertions in human disease.** *Mob DNA* 2016, **7:**9.
7. Ewing AD, Ballinger TJ, Earl D, Harris CC, Ding L, Wilson RK, Haussler D, Platform BIGSaAPa: **Retrotransposition of gene transcripts leads to structural variation in mammalian genomes.** *Genome Biol* 2013, **14:**R22.
8. Yoder JA, Walsh CP, Bestor TH: **Cytosine methylation and the ecology of intragenomic parasites.** *Trends Genet* 1997, **13:**335-340.
9. Daniel C, Behm M, Öhman M: **The role of Alu elements in the cis-regulation of RNA processing.** *Cell Mol Life Sci* 2015, **72:**4063-4076.
10. Economou-Pachnis A, Tsichlis PN: **Insertion of an Alu SINE in the human homologue of the Mlvi-2 locus.** *Nucleic Acids Res* 1985, **13:**8379-8387.
11. Kazazian HH, Wong C, Youssoufian H, Scott AF, Phillips DG, Antonarakis SE: **Haemophilia A resulting from de novo insertion of L1 sequences represents a novel mechanism for mutation in man.** *Nature* 1988, **332:**164-166.
12. Payer LM, Burns KH: **Transposable elements in human genetic disease.** *Nat Rev Genet* 2019, **20:**760-772.
13. Teugels E, De Brakeleer S, Goelen G, Lissens W, Sermijn E, De Grève J: **De novo Alu element insertions targeted to a sequence common to the BRCA1 and BRCA2 genes.** *Hum Mutat* 2005, **26:**284.
14. Peixoto A, Santos C, Pinheiro M, Pinto P, Soares MJ, Rocha P, Gusmão L, Amorim A, van der Hout A, Gerdes AM, et al: **International distribution and age estimation of the Portuguese BRCA2 c.156_157insAlu founder mutation.** *Breast Cancer Res Treat* 2011, **127:**671-679.
15. De Brakeleer S, De Grève J, Lissens W, Teugels E: **Systematic detection of pathogenic alu element insertions in NGS-based diagnostic screens: the BRCA1/BRCA2 example.** *Hum Mutat* 2013, **34:**785-791.
16. Qian Y, Mancini-DiNardo D, Judkins T, Cox HC, Brown K, Elias M, Singh N, Daniels C, Holladay J, Coffee B, et al: **Identification of pathogenic retrotransposon insertions in cancer predisposition genes.** *Cancer Genet* 2017, **216-217:**159-169.
17. Shahi RB, De Brakeleer S, Caljon B, Pauwels I, Bonduelle M, Joris S, Fontaine C, Vanhoeij M, Van Dooren S, Teugels E, De Grève J: **Identification of candidate cancer predisposing variants by performing whole-exome sequencing on index patients from BRCA1 and BRCA2-negative breast cancer families.** *BMC Cancer* 2019, **19:**313.
18. Keane TM, Wong K, Adams DJ: **RetroSeq: transposable element discovery from next-generation sequencing data.** *Bioinformatics* 2013, **29:**389-390.

19. Robinson JT, Thorvaldsdóttir H, Winckler W, Guttman M, Lander ES, Getz G, Mesirov JP: **Integrative genomics viewer.** *Nat Biotechnol* 2011, **29:**24-26.
20. Stewart C, Kural D, Strömberg MP, Walker JA, Konkel MK, Stütz AM, Urban AE, Grubert F, Lam HY, Lee WP, et al: **A comprehensive map of mobile element insertion polymorphisms in humans.** *PLoS Genet* 2011, **7:**e1002236.
21. Witherspoon DJ, Zhang Y, Xing J, Watkins WS, Ha H, Batzer MA, Jorde LB: **Mobile element scanning (ME-Scan) identifies thousands of novel Alu insertions in diverse human populations.** *Genome Res* 2013, **23:**1170-1181.
22. Chen LL, Yang L: **ALUternative Regulation for Gene Expression.** *Trends Cell Biol* 2017, **27:**480-490.
23. Spengler RM, Oakley CK, Davidson BL: **Functional microRNAs and target sites are created by lineage-specific transposition.** *Hum Mol Genet* 2014, **23:**1783-1793.
24. Luedi PP, Dietrich FS, Weidman JR, Bosko JM, Jirtle RL, Hartemink AJ: **Computational and experimental identification of novel human imprinted genes.** *Genome Res* 2007, **17:**1723-1730.
25. Greally JM: **Short interspersed transposable elements (SINEs) are excluded from imprinted regions in the human genome.** *Proc Natl Acad Sci U S A* 2002, **99:**327-332.
26. Wang J, Song L, Grover D, Azrak S, Batzer MA, Liang P: **dbRIP: a highly integrated database of retrotransposon insertion polymorphisms in humans.** *Hum Mutat* 2006, **27:**323-329.
27. Sjöblom T, Jones S, Wood LD, Parsons DW, Lin J, Barber TD, Mandelker D, Leary RJ, Ptak J, Silliman N, et al: **The consensus coding sequences of human breast and colorectal cancers.** *Science* 2006, **314:**268-274.
28. Olsen TK, Panagopoulos I, Gorunova L, Micci F, Andersen K, Kilen Andersen H, Meling TR, Due-Tønnessen B, Scheie D, Heim S, Brandal P: **Novel fusion genes and chimeric transcripts in ependymal tumors.** *Genes Chromosomes Cancer* 2016, **55:**944-953.
29. Sun SC, Ma D, Li MY, Zhang RX, Huang C, Huang HJ, Xie YZ, Wang ZJ, Liu J, Cai DC, et al: **Mutations in C1orf194, encoding a calcium regulator, cause dominant Charcot-Marie-Tooth disease.** *Brain* 2019, **142:**2215-2229.
30. van de Kooij B, Creixell P, van Vlimmeren A, Joughin BA, Miller CJ, Haider N, Simpson CD, Linding R, Stambolic V, Turk BE, Yaffe MB: **Comprehensive substrate specificity profiling of the human Nek kinome reveals unexpected signaling outputs.** *Elife* 2019, **8**.
31. Chivukula RR, Montoro DT, Leung HM, Yang J, Shamseldin HE, Taylor MS, Dougherty GW, Zariwala MA, Carson J, Daniels MLA, et al: **A human ciliopathy reveals essential functions for NEK10 in airway mucociliary clearance.** *Nat Med* 2020, **26:**244-251.
32. Mello SS, Valente LJ, Raj N, Seoane JA, Flowers BM, McClendon J, Bieging-Rolett KT, Lee J, Ivanochko D, Kozak MM, et al: **A p53 Super-tumor Suppressor Reveals a Tumor Suppressive p53-Ptpn14-Yap Axis in Pancreatic Cancer.** *Cancer Cell* 2017, **32:**460-473.e466.
33. Liu X, Sun L, Gursel DB, Cheng C, Huang S, Rademaker AW, Khan SA, Yin J, Kiyokawa H: **The non-canonical ubiquitin activating enzyme UBA6 suppresses epithelial-mesenchymal transition of mammary epithelial cells.** *Oncotarget* 2017, **8:**87480-87493.
34. Cai X, Wang X, Cao C, Gao Y, Zhang S, Yang Z, Liu Y, Zhang X, Zhang W, Ye L: **HBXIP-elevated methyltransferase METTL3 promotes the progression of breast cancer via inhibiting tumor suppressor let-7g.** *Cancer Lett* 2018, **415:**11-19.
35. Lan Q, Liu PY, Haase J, Bell JL, Hüttelmaier S, Liu T: **The Critical Role of RNA m.** *Cancer Res* 2019, **79:**1285-1292.
36. Gupta P, Li YR: **Upf proteins: highly conserved factors involved in nonsense mRNA mediated decay.** *Mol Biol Rep* 2018, **45:**39-55.
37. Ranjan A, Iyer SV, Iwakuma T: **Suppressive roles of A3AR and TMIGD3 i1 in osteosarcoma malignancy.** *Cell Cycle* 2017, **16:**903-904.

38. Mollenhauer J, Wiemann S, Scheurlen W, Korn B, Hayashi Y, Wilgenbus KK, von Deimling A, Poustka A: **DMBT1, a new member of the SRCR superfamily, on chromosome 10q25.3-26.1 is deleted in malignant brain tumours.** *Nat Genet* 1997, **17:**32-39.
39. Wu W, Kemp BL, Proctor ML, Gazdar AF, Minna JD, Hong WK, Mao L: **Expression of DMBT1, a candidate tumor suppressor gene, is frequently lost in lung cancer.** *Cancer Res* 1999, **59:**1846-1851.
40. Braidotti P, Nuciforo PG, Mollenhauer J, Poustka A, Pellegrini C, Moro A, Bulfamante G, Coggi G, Bosari S, Pietra GG: **DMBT1 expression is down-regulated in breast cancer.** *BMC Cancer* 2004, **4:**46.
41. Sorek R, Ast G, Graur D: **Alu-containing exons are alternatively spliced.** *Genome Res* 2002, **12:**1060-1067.
42. Ding J, Wu W, Yang J, Wu M: **Long non-coding RNA MIF-AS1 promotes breast cancer cell proliferation, migration and EMT process through regulating miR-1249-3p/HOXB8 axis.** *Pathol Res Pract* 2019, **215:**152376.
43. Wagner K, Hemminki K, Grzybowska E, Bermejo JL, Butkiewicz D, Pamula J, Pekala W, Försti A: **Polymorphisms in the growth hormone receptor: a case-control study in breast cancer.** *Int J Cancer* 2006, **118:**2903-2906.
44. Canzian F, Cox DG, Setiawan VW, Stram DO, Ziegler RG, Dossus L, Beckmann L, Blanché H, Barricarte A, Berg CD, et al: **Comprehensive analysis of common genetic variation in 61 genes related to steroid hormone and insulin-like growth factor-I metabolism and breast cancer risk in the NCI breast and prostate cancer cohort consortium.** *Hum Mol Genet* 2010, **19:**3873-3884.
45. Rudd MF, Webb EL, Matakidou A, Sellick GS, Williams RD, Bridle H, Eisen T, Houlston RS, Consortium G: **Variants in the GH-IGF axis confer susceptibility to lung cancer.** *Genome Res* 2006, **16:**693-701.
46. Tchatchou S, Riedel A, Lyer S, Schmutzhard J, Strobel-Freidekind O, Gronert-Sum S, Mietag C, D'Amato M, Schlehe B, Hemminki K, et al: **Identification of a DMBT1 polymorphism associated with increased breast cancer risk and decreased promoter activity.** *Hum Mutat* 2010, **31:**60-66.
47. Gao C, Devarajan K, Zhou Y, Slater CM, Daly MB, Chen X: **Identifying breast cancer risk loci by global differential allele-specific expression (DASE) analysis in mammary epithelial transcriptome.** *BMC Genomics* 2012, **13:**570.
48. Blackburn AC, Hill LZ, Roberts AL, Wang J, Aud D, Jung J, Nikolcheva T, Allard J, Peltz G, Otis CN, et al: **Genetic mapping in mice identifies DMBT1 as a candidate modifier of mammary tumors and breast cancer risk.** *Am J Pathol* 2007, **170:**2030-2041.
49. Ahmed S, Thomas G, Ghoussaini M, Healey CS, Humphreys MK, Platte R, Morrison J, Maranian M, Pooley KA, Luben R, et al: **Newly discovered breast cancer susceptibility loci on 3p24 and 17q23.2.** *Nat Genet* 2009, **41:**585-590.
50. Decker B, Allen J, Luccarini C, Pooley KA, Shah M, Bolla MK, Wang Q, Ahmed S, Baynes C, Conroy DM, et al: **Targeted Resequencing of the Coding Sequence of 38 Genes Near Breast Cancer GWAS Loci in a Large Case-Control Study.** *Cancer Epidemiol Biomarkers Prev* 2019, **28:**822-825.
51. Babaian A, Mager DL: **Endogenous retroviral promoter exaptation in human cancer.** *Mob DNA* 2016, **7:**24.
52. Jang HS, Shah NM, Du AY, Dailey ZZ, Pehrsson EC, Godoy PM, Zhang D, Li D, Xing X, Kim S, et al: **Transposable elements drive widespread expression of oncogenes in human cancers.** *Nat Genet* 2019, **51:**611-617.
53. Guevara-Aguirre J, Guevara A, Palacios I, Pérez M, Prócel P, Terán E: **GH and GHR signaling in human disease.** *Growth Horm IGF Res* 2018, **38:**34-38.
54. Mir AA, Philippe C, Cristofari G: **euL1db: the European database of L1HS retrotransposon insertions in humans.** *Nucleic Acids Res* 2015, **43:**D43-47.

55. Payer LM, Steranka JP, Yang WR, Kryatova M, Medabalimi S, Ardeljan D, Liu C, Boeke JD, Avramopoulos D, Burns KH: **Structural variants caused by A*lu* insertions are associated with risks for many human diseases.** *Proc Natl Acad Sci U S A* 2017, **114:**E3984-E3992.
56. Li H: **Toward better understanding of artifacts in variant calling from high-coverage samples.** *Bioinformatics* 2014, **30:**2843-2851.
57. Rishishwar L, Mariño-Ramírez L, Jordan IK: **Benchmarking computational tools for polymorphic transposable element detection.** *Brief Bioinform* 2017, **18:**908-918.
58. Hubley R, Finn RD, Clements J, Eddy SR, Jones TA, Bao W, Smit AF, Wheeler TJ: **The Dfam database of repetitive DNA families.** *Nucleic Acids Res* 2016, **44:**D81-89.

to be added to ref35 (bold): …role of RNA m**6A Methylation in Cancer.**

(not accepted by EndNote)

688 **FIGURES (titles and legends)**

689

690 Figure 1

691 Title: Schematic representation of the "discordantly mapped read pairs" used for the detection of
692 polymorphic retrotransposons

693 Legend: After genome fragmentation (broken arrows), size selected DNA fragments are
694 sequenced from both ends (paired-end sequencing). DNA fragments having one breakpoint in a
695 gene and the other breakpoint in a retrotransposon not included in the reference human genome
696 will generate read pairs (grey filled arrows) that do not map at nearby positions on the reference
697 genome after alignment. The discordantly mapped read pairs obtained by analysis of the full
698 exome of a patient (traceable in the corresponding BAM file) are further selected for the
699 presence of a long polyA stretch in one of the mate reads. An additional landmark for
700 retrotransposition is the presence of a target site duplication (TSD) flanking the transposon.

701

702

703 Figure 2

704 Title: Screenshots of IGV outputs visualizing the Alu element insertion in the positive control
705 sample

706 Legend: The screenshots are restricted to the genomic region where the Alu element insertion
707 occurred (c.1739_1740insAlu in *BRCA1*) in the positive control sample. The BAM file used for
708 IGV visualization was generated from WES data obtained with the exome capture kit SeqCap EZ

709 Exome v3.0 from Roche. Group alignment is by chromosome of mate. Note the presence of a
710 high number of reads (22) whose mate reads are located on another chromosome (encircled and
711 labelled "A"). All those BRCA1 specific reads point in the same direction, the 3' extremity of
712 the Alu insertion that ends with a long polyA stretch (3 of these 22 reads already end with a
713 small polyA stretch). Consequently, the mates of these 22 reads have a high probability to
714 contain a long polyA stretch and to be picked up with our detection strategy. Five such
715 discordantly mapped read pairs are sufficient to retain this particular genomic region as a
716 candidate insertion site. Note also that a number of correctly mapped read pairs (labelled "B" and
717 "C") start with a sequence that do not correspond to the *BRCA1* sequence. The reads labelled
718 "B" confirm the presence (and position) of a polyA stretch adjacent to the *BRCA1* sequence,
719 while the reads labelled "C" allow the identification of the inserted sequence most upstream of
720 the polyA stretch, in this case an Alu element. Inserted retrotransposon sequences can be
721 identified making use of the Dfam [58] database (https://dfam.org/home), processed pseudogenes
722 with BLAST (https://blast.ncbi.nlm.nih.gov/Blast.cgi). Finally, and characteristic for
723 retrotransposition events, the inserted element is flanked by a short repeated sequence (TSD,
724 17bp long in this case) as is indicated with label "D". Often, a sharp increase of the coverage at
725 the level of the TSD is observed (less pronounced in this example, see label "E").

726

727

728 Figure 3

729 Title: Alu element insertions in *UPF2* and *NEK10* do not induce allelic up or down regulation

Legend: Sanger sequencing experiments were performed on RNA material obtained from blood leucocytes. The chromatograms show a nucleotide region containing a polymorphic position (a SNP, indicated by an arrow) for which all tested samples were heterozygous at the genomic level. (A) In addition to be heterozygous for c.1539A>C (rs11595168), all 5 samples were also heterozygous for the Alu insertion in the intronic region of *UPF2* (c.3408+98_+111insAlu). The c.1539C allele is very rare and was not detected among available control samples. (B) In addition to be heterozygous for c.1674A>G (rs674303), 1 of the 4 samples was also heterozygous for the Alu insertion in the intronic region of *NEK10* (c.26+891_908insAlu).

Figure 4

Title: Alu element insertions in *GHR* and *PTPN10* modulate allelic expression

Legend: Sanger sequencing experiments performed on RNA material obtained from blood leucocytes. The chromatograms show a nucleotide region containing a polymorphic position (arrow) for which the tested samples were heterozygous at the genomic level. (A) In addition to be heterozygous for c.558A>G (rs2397118), 3 of the 5 samples were also heterozygous for the Alu insertion in the 3'UTR of *GHR* (c.*+413_+422insAlu). Allele silencing is observed in all Alu mutation carriers. (B) In addition to be heterozygous for c.978A>G (rs7550799), 2 of the 5 samples were also heterozygous for the Alu insertion in the intronic region of *PTPN14* (c.10066+35_+44insAlu). Note that the two Alu mutation carriers express both alleles well, while one control sample (sample *PTPN14*_ctrl1) expresses almost exclusively the G allele, the 2 other control samples showing a deficit in the G allele.

752

753

754 Figure 5

755 Title: IGV visualization of the control Alu insertion using BAM file generated with the Agilent
756 kit

757 Legend: Screenshots of IGV outputs restricted to the genomic region where the Alu element
758 insertion occurred (c.1739_1740insAlu in *BRCA1*) in the positive control sample. The BAM file
759 used for IGV visualization was generated from WES data obtained with the SureSelect Human
760 All Exon V6 kit (exome capture kit) from Agilent. Group alignment is by chromosome of mate.
761 Note that this exome capture kit generates much less discordantly mapped read pairs than the kit
762 from Roche (2 versus 22, compare with Figure 2). Accordingly, the required number (five) of
763 discordantly mapped read pairs containing a long polyA track will not be reached and the
764 insertion will not be revealed with our detection strategy. Note that all other characteristics
765 observed for a retrotransposon insertion when using the exome capture kit from Roche (see
766 Figure 2) are also observed when using the kit from Agilent.

767

768 Table 1: List with the 18 high confidence retrotransposition mediated insertions detected in 65
769 familial BC patients

Targeted gene (region)	Location TSD (RefSeq); orientation of the insertion compared to the targeted gene	Transposed sequence	5' extremity of the transposed sequence[a]	# carriers (cl_5)[b]	# carriers (cl_3)[c]	# carriers IGV[d]	reported in dbRIP?
BRCA1 (exon)	c.1723_1739 (NM_007294); sense	Alu	positive control	1	1	1	yes
GHR (3'UTR)	c.*+413_+422 (NM_000163.5); antisense	Alu[e]	1_42 of AluYe6	3	3	5	yes
GSTA5 (promoter)	1,3 Kb up transcription start (NM_153699.1); antisense	Alu[e]	1_59 of AluYb9	4	4	4	yes
METTL3 (intron)	c.1456+69_+84 (NM_019852.5); antisense	Alu[e]	1_58 of AluYd8	1	1	1	no
NEK10 (intron)	c.26+891_+908 (CCDS77713); antisense	Alu[e]	2_53 of AluYe6	1	1	3	no
PTPN14 (intron)	c.10066+35_+44 (NM_005401.5);sense	Alu[e]	1_57 of AluYd8	3	4	4	no
UPF2 (intron)	c.3408+98_+111 (NM_080599.2); antisense	Alu[e]	2_53 of AluYe6	3	3	3	no
ZNF442 (exon)	c.1402_1413 (NM_030824.3); antisense	Alu[e]	1_47 of AluSx3	1	1	1	no
TMIGD3 (intron)	c.458-623_-638 (NM_020683.7); antisense	Alu	2_55 of AluYe6	1	4	7	yes
intergenic	closest gene at 10kb (GPR42)	Alu	1_57 of AluYd8	2	2	2	no
intergenic	2 genes at 30Kb (MIF-AS1 & GSTT2B)	Alu	1_57 of AluYb9	1	5	5	yes
HSD17B12 (3'UTR)	c.*+642_+650 (NM_016142.3); antisense	Alu	1_46 of AluYe6	1	4	29	yes
intergenic	closest gene at 85kb (CLVS1)	L1	2247_2296 of L1P1_orf2	1	4	5	no
DMBT1 (intron)	c.1459+48_+63 (NM_007329.2); antisense	L1	4_54 of L1HS	1	1	1	no
UBA6 (intron)	c.1097+17_+25 (NM_018227.6); sense	SVA	731_778 of SVA_F	1	1	1	no
C1orf194 (exon)	c.58_70 (NM_001122961.1); sense	UQCR10	starts at c.-15 (NM_013387.4)	1	4	7	pseudogene
PSMA7 (intron)	c.654+95_+107 (NM_002792.4); antisense	MRPL50	starts at c.-7 (NM_019051.3)	1	1	1	pseudogene
DPP10 (intron)	c.442-70581_-70595 (NM_001321907.1) ; antisense	SET	starts at c.*+199 (NM_003011)	1	4	35	pseudogene

770

771 Strong candidate integration sites are retained when generated by clusters counting at least 5
772 polyA containing discordantly mapped read pairs, when present in less than 10% of the samples,
773 and when a TSD is deducible upon IGV inspection in at least one patient. [a] indicates the number
774 of nucleotides available to identify retrotransposon type (using the Dfam database [58]). As only
775 about 50 nucleotides are available for transposon identification, it was not possible to define sub-
776 classes. [b] indicates the number of patients (out of 65) who carry the mutation based on clusters
777 counting at least 5 discordantly mapped read pairs. [c] indicates the number of patients who carry
778 the same mutation based on clusters counting at least 3 discordantly mapped read pairs. [d]
779 indicates the number of patients harboring the same mutation based upon IGV inspection. Note
780 that for two insertions (SET in *DPP10* and Alu in *HSD17B12*) a much higher number of carriers
781 is revealed upon IGV inspection. This discrepancy results from the poor coverage at sequencing.
782 [e] indicates the Alu insertions for which a genomic hemi-nested PCR has been developed and
783 applied for validation (see Methods).

784

785 Table 2: Results from insAlu genotyping experiments performed on 710 non related familial BC
786 patients

Alu targeted gene	# carriers out of 710
UPF2	107
PTPN14	10
GHR	17
ZNF442	1
METTL3	1

787 The primers used for mutation specific PCR amplification are presented in Table 6

788

789

790

791

792

793 Table 3: List with the 14 polyA associated insertions for which a TSD could not be defined.

Targeted gene (region)	Insertion type	Position of insertion in cDNA (RefSeq)	Position of insertion in hg19	Retrotransposon sequence in mate?	# carriers cl_5	# carriers cl_3	reported in dbRIP?
ANAPC16 (3'UTR)	polyA	c.*+397 (NM_001242546.1)	chr10:73993271	no	2	2	yes (Alu)
ARHGAP1 (intron)	polyA	c.317+71 (NM_004308)	chr11:46709653	yes (Alu)	1	1	no
AUH (intron)	polyA	c.599-122 (NM_001698)	ch9:94058481	yes (L1)	1	4	yes (L1)
CLEC1B (intron)	polyA	c.438+306 (NM_016509)	ch12:10149139	no	1	2	no
DHRS1 (intron)	polyA	c.374+111 (NM_138452)	chr14:24765604	yes (Alu)	1	1	no
DYNC2H1 (intron)	polyA	c.6139+43 (NM_001377)	chr11:103048592	yes (Alu)	1	1	yes (Alu)
ETF1 (3'UTR)	polyA	c.*+2210 (NM_004730)	ch5:137841784	no	1	1	no
GCNT1 (3'UTR)	polyA	c.*+2545 (NM_001490)	chr9:79121129	yes (Alu)	1	1	no
GSAP (intron)	polyA	c.1491+495 (NM_017439)	chr7:76980766	yes (Alu)	1	1	yes (Alu)
MEOX2 (intron)	polyA	c.690+95 (NM_005924)	chr:7:15666276	yes (Alu)	1	1	yes (Alu)
MIER1 (3'UTR)	polyA	c.*+1193 (NM_020948)	chr1:67453349	no	1	1	no
USP38 (intron)	polyA	c.1210-89 (NM_032557)	chr4:144127097	yes (Alu)	1	1	yes (Alu)
intergenic	polyA	LINC0251 at 46kb	chr6:114017537	no	3	4	no
intergenic	polyA	SPIN1 at 6,1kb	chr9:91099726	no	1	3	yes (Alu)

794 Note that for 8 of the 14 polyA containing insertion sites, a partial retrotransposon sequence
795 could be traced in the mate of at least one discordantly mapped read upon IGV inspection (5th
796 column). Screening the database for Retrotransposition Insertion Polymorphisms in Human
797 (dbRIP) at the corresponding positions confirmed the presence of a retrotransposon at 7 of the 14
798 positions (8th column).

799

800 Table 4: Number of hits obtained in PubMed when searching for the polyA targeted genes.

PubMed domain	title	title/abstract	title/abstract	title/abstract
Search terms used	**"all gene names"**	**"all gene names"**	**"all gene names" AND "cancer"**	**"all gene names" AND "breast cancer"**
gene (synonyms)[a]				
ANAPC16 (APC16, C10orf104, CENP-27, FLJ33728, bA570G20.3)	5	5	0	0
ARHGAP1 (CDC42GAP, ~~RhoGAP~~, p50rhoGAP)	31	93	15	4
~~AUH~~	-	-	-	-
CLEC1B (CLEC2)	9	49	6	0
DHRS1 (FLJ25430, MGC20204, SDR19C1)	1	4	1	0
DYNC2H1 (DHC1b, DHC2, DNCH2, DYH1B, hdhc11)	26	86	4	0
ETF1 (~~ERF~~, ERF1, RF1, SUP45L1, TB3-1)	185	845	21	5
GCNT1 (C2GNT, NACGT2, NAGCT2)	8	124	35	1
GSAP (LOC54103, ~~PION~~)	6	31	1	0
MEOX2 (GAX, ~~MOX2~~)	85	254	22	1
MIER1 (KIAA1610, MI-ER1, hMI-ER1)	10	15	2	2
USP38 (HP43.8KD, KIAA1891)	6	10	3	1
intergenic: LINC0251 at 46kb	0	0	0	0
intergenic; SPIN1 at 6kb (~~SPIN~~, TDRD24)	18	34	14	4

801 This table shows the number of hits obtained in PubMed when using as search term a specific
802 gene or its synonym (= "all gene names") in combination with "cancer" or "breast cancer" and
803 when restricting the search to particular domains (title or abstract). [a]gene names generating
804 excessive number of false positive hits were removed (strikethrough). Search was performed on
805 14/01/2020

806

807 Table 5: Number of hits obtained in PubMed when searching for high confidence targeted genes.

PubMed domain	title	title/abstract	title/abstract	title/abstract
Search terms used	**"all gene names"**	**"all gene names"**	**"all gene names" AND "cancer"**	**"all gene names" AND "breast cancer"**
gene (synonyms)[a]				
BRCA1 (BRCC1, FANCS, PPP1R53, RNF53); positive control	6503	14198	11505	7402
GHR (GHBP)	208	2416	129	35
GSTA5	2	29	7	2
METTL3 (~~M6A~~, MT-A70, Spo8)	80	251	65	6
NEK10 (FLJ32685)	1	17	11	8
PTPN14 (PEZ)	33	98	37	6
UPF2 (DKFZP434D222, KIAA1408, RENT2, smg-3)	32	189	5	0
ZNF442 (FLJ14356)	0	0	0	0
TMIGD3 (AD026)	2	2	1	0
intergenic: GPR42 at 10 kb (FFAR3L, GPR41L, GPR42P)	2	4	0	0
intergenic: MIF-AS1 at 30 kb (LOC284889, MIF-AS)	4	5	2	1
intergenic: GSTT2B at 30kb (GSTT2P)	2	8	2	0
intergenic: CLVS1 at 85kb (C6orf212L, CRALBPL, MGC34646, RLBP1L1)	2	7	1	0
DMBT1 (GP340, Gp-340, ~~SALSA~~, hensin, muclin, vomeroglandin)	166	389	68	7
UBA6 (FLJ10808, UBE1L2)	14	32	5	1
C1orf194	1	2	0	0
PSMA7 (~~C6~~, ~~HSPC~~, RC6-1, XAPC7)	19	60	18	0
UQCR10 (HSPC051, QCR9, UCCR7.2, UCRC) transcript in C1orf194	3	35	4	0
MRPL50 (FLJ20493, MRP-L50) transcript in PSMA7	0	2	0	0

808 This table shows the number of hits obtained in PubMed when using as search term a specific
809 gene or its synonym (= "all gene names") in combination with "cancer" or "breast cancer" and
810 when restricting the search to specific domains (title or abstract). [a]gene names generating
811 excessive number of false positive hits were removed (strikethrough). Search was performed on
812 13/01/2020.

813

814

815 Table 6: Primers used for the detection of 7 Alu element insertions in genomic DNA

Primer name	Primer sequence	wt fragment size (bp)
PTPN14/Gen/F1	GTGTGGTGAGCACTACTCGG	
PTPN14/Gen/R1	CTGACAGTCTAGGCCTTCCAC	205
GHR/Gen/F1	AAATCAGGTGGCTTTTGCGG	
GHR/Gen/R1	AGAGGGGTCATACCAACTGC	275
GSTA5/Gen/F1	TGGTATAAACGGTGGTGGCA	
GSTA5/Gen/R1	TAGCTTCACAACAGGCACAA	286
NEK10/DNA/F1	AATGGCAGCTTACTTCACGG	
NEK10/DNA/R1	AGGAATTGTCTTCTCACCTTCTTT	240
UPF2/E17/F	GGAAAATGAAACCGATGAAGA	
UPF2/I17/R	GGGCAAAGCCTTTTAGTATTGA	272
METTL3/Gen/F1	CCTGTCTGCTCAGAAAACTCG	
METTL3/Gen/R1	AGCGGATATCACAACAGATCCA	249
ZNF442/Gen/F1	GCCTTCCGTATTTCTAGTTCCC	
ZNF442/Gen/R1	TTTCAGCCATGTGAGTCCTTCT	220
Alu/Rev	TTTTTAGTAGAGACGGGGTTTC	

816

817

818 Table 7: Primers used for genotyping at polymorphic positions (for RNA study)

Primer name	Primer sequence	fragment size (bp)	SNP
PTPN14/ex11/F	CCTTCCCTTGTCTATCTGGTCTTT		rs7550799
PTPN14/ex11/R	CAAGGGGGACAAAACGGGTG	298	c.978A>G; p.Arg326=
GHR/ex6/F	CCACCCATTGCCCTCAACTG		rs6179
GHR/ex6/R	AGGTGTAGCAACATCTTACCATTT	187	c.558A>G; p.Gly186=
GSTA5/i2/F	GGGTGGGTTTCATAGACACTTCATA		rs2397118
GSTA5/RNA/R1	AGGGCTCTCTCCTTCATGTCT	183	c.163G>A; p.Val55Ile
NEK10/ex20/F1	AGGTTAGAAAGCATAGTGGTCAAA		rs674303
NEK10/ex20/R1	TGGACAAGAGCACCACAACT	222	c.1674A>G; p.Gly558=
UPF2/ex6/F1	ACTTTTGTGCAGCAGGATTTTCA		rs11595168
UPF2/ex6/R1	GGCAAGAGCTCTGTGTGTAA	274	c.1539A>C; p.Ser513=

819

820

821 Table 8: Primers used for cDNA amplification (and Sanger sequencing)

Primer name	Primer sequence	fragment size (bp)
PTPN14/RNA/F1	GTTGTTTGCCACACGACAC	
PTPN14/RNA/R1	AGTTGACGCTGTGAACGCTA	308
GHR/RNA/S1	ATTGCCCTCAACTGGACTTTA	
GHR/RNA/R1	TGGATCTCACACGCACTTCA	241
GSTA5/RNA/F1	GCTGCAGCTGGAGTAGAGTT	
GSTA5/RNA/R1	AGGGCTCTCTCCTTCATGTCT	203
NEK10/RNA/F2	CAGAGCCTTGAGATTTCTCTTCAG	
NEK10/RNA/R2	TTACGCTGCTGTCTCGATCTTT	386
UPF2/RNA/F1	TTTGTCCCAGCCATCTTGTT	
UPF2/RNA/R1	GTGCTGGCTTCCTCATCTTC	250

822

823

824 **ADDITIONAL MATERIAL > INFORMATION LIST**

825

826 Additional file 1 (Excel file)

827 Title: Strong candidates retrotransposon mediated insertion sites

828 Description: This table lists all strong candidate insertion sites detected with the RetroSeq
829 software (minimum 5 discordantly mapped read pairs pointing to the same genomic location)
830 and further filtered using Excel software to remove false positives and insertions occurring in
831 more than 10% of the investigated patient samples.

832

833 Additional file 2 (Word file)

834 Title: Retrotransposon targeted genes with no TSD identified

835 Description: For each gene presumably targeted by a retrotransposition event that could not be
836 confirmed by the presence of a TSD, a short description is given. The gene/protein descriptions
837 provided by "Entrez Gene Summary" (https://www.ncbi.nlm.nih.gov/gene), by "GeneCards
838 Summary" (https://www.genecards.org) and by "UniProtKB/Swiss-Prot Summary"
839 (https://uniprot.org) are presented, when available.

840

841 Additional file 3 (Word file)

842 Title: Retrotransposon targeted genes with TSD identified

Description: For each gene targeted by a retrotransposition event that could be confirmed by the presence of a TSD, a short description is given. The gene/protein descriptions provided by "Entrez Gene Summary" (https://www.ncbi.nlm.nih.gov/gene), by "GeneCards Summary" (https://www.genecards.org) and by "UniProtKB/Swiss-Prot Summary" (https://uniprot.org) are presented, when available.

Additional file 4 (Excel file)

Title: RetroSeq generated list of anchor reads when using the positive control sample

Description: This table lists all discordantly mapped read pairs (19.674 in total) selected by the RetroSeq software when analyzing the positive control sample (patient harboring the c.1739_1740insAlu mutation in BRCA1). The input BAM file was generated using the exome capture kit SeqCap EZ Exome v3.0 from Roche for library preparation. To be selected, one read of the discordantly mapped read pair must contain a long polyA stretch, while the position of the mate of this read on the reference genome is used for ordering the RefSeq selected read pairs.

Additional file 5 (Excel file)

Title: Excel file for cluster calculation

Description: This pre-formated Excel file can be used to extract potential retrotransposon insertion sites from lists generated with the RetroSeq software (e.g. the list presented in Additional file 4)

Additional file 6 (Excel file)

Title: Output of cluster calculation for the positive control sample

Description: This table lists all potential retrotransposon integration sites observed in the positive control sample (641 in total). Integration sites are retained only when 3 or more anchor reads cluster in the same genomic interval (max 300bp long).

Additional file 7 (Excel file)

Title: Excel file for cluster filtering

Description: This pre-formated Excel file allows further filtering of the potential retrotransposon integration sites (output of Additional file 5). Highly recurrent integration sites (occurring in more than 10% of the investigated population) or false positives are removed during this filtering step.

Figure 1

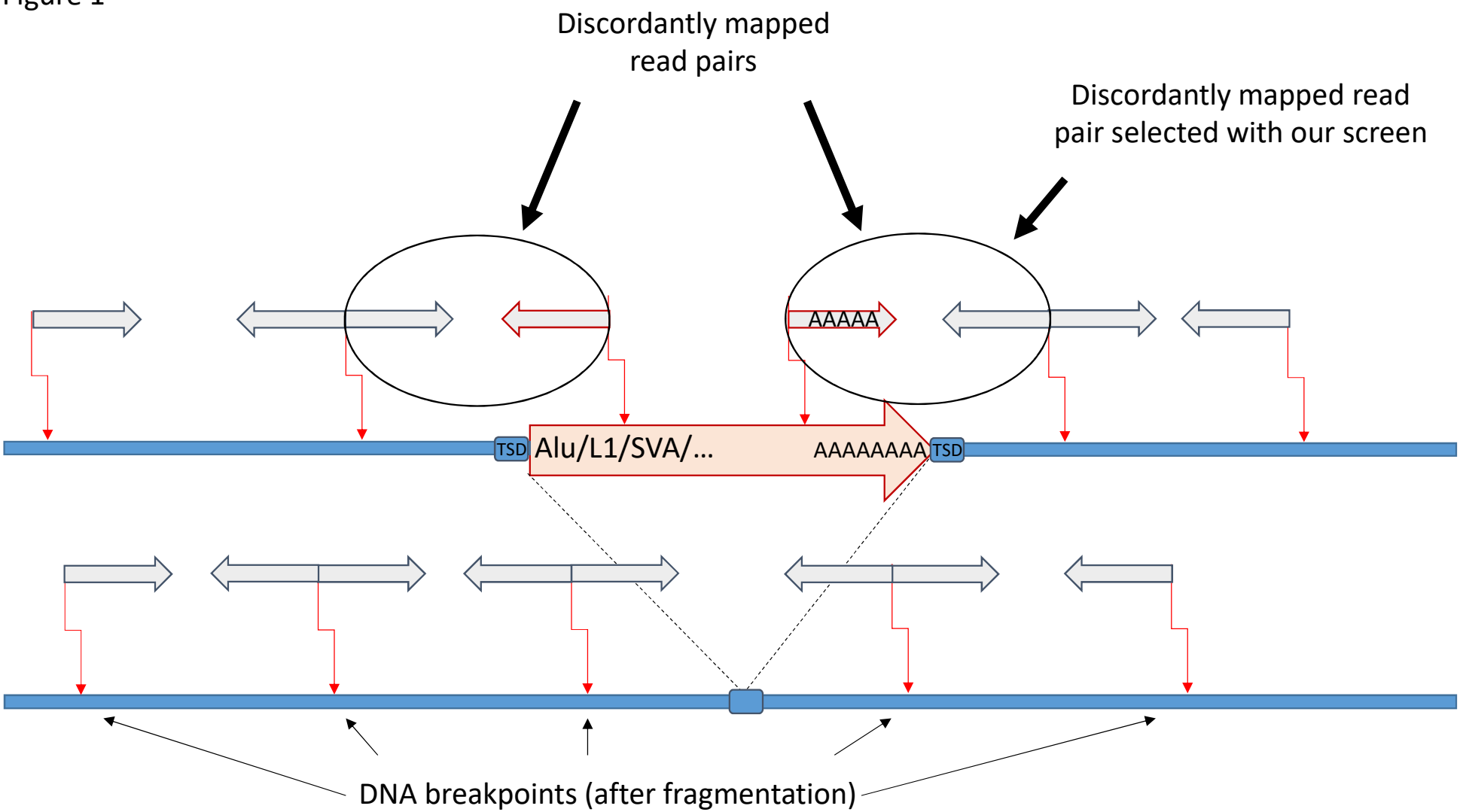
Discordantly mapped
read pairs
Discordantly mapped read
pair selected with our screen
AAAAA
TSD
Alu/L1/SVA/…
AAAAAAAA
TSD
DNA breakpoints (after fragmentation)

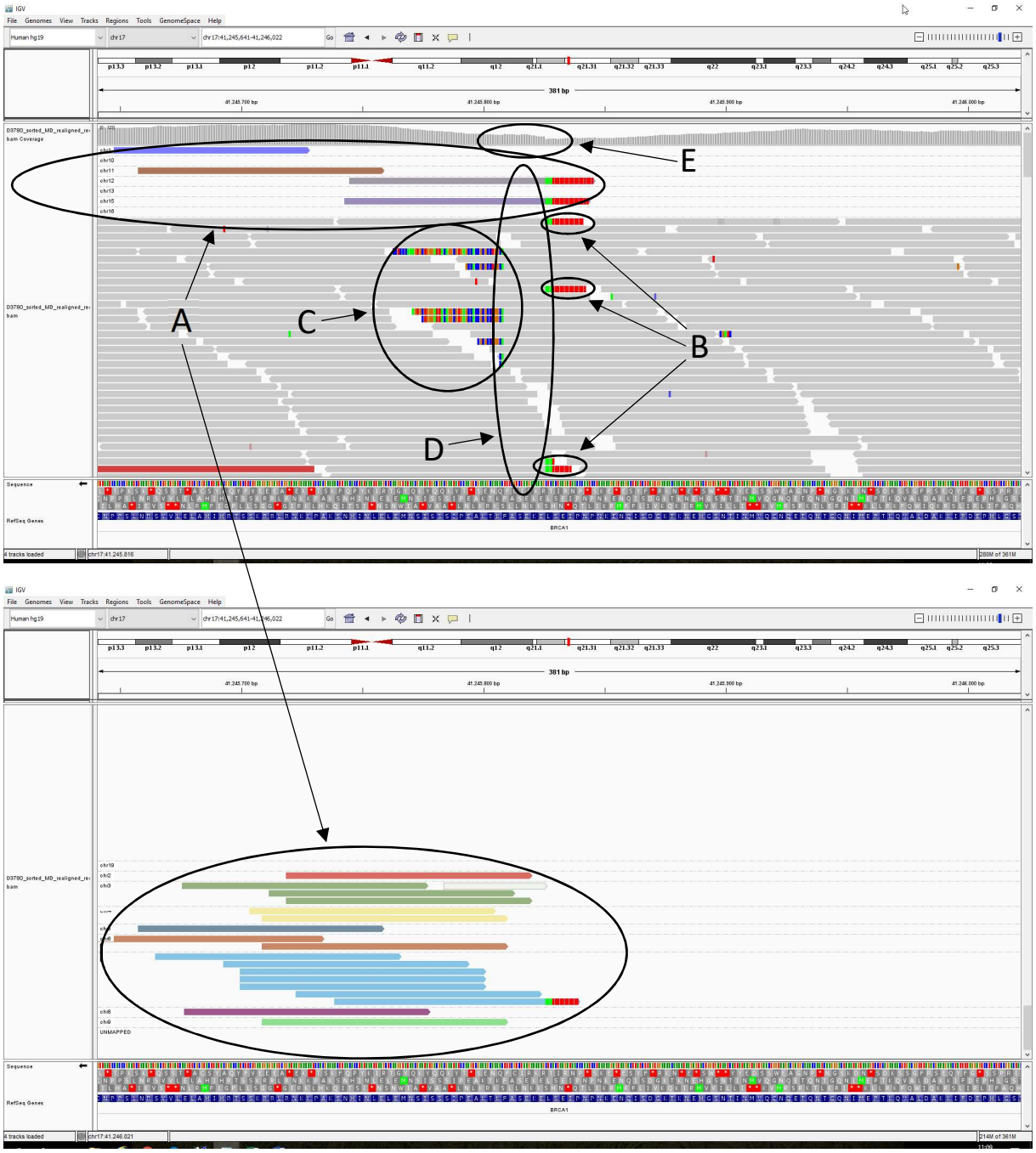

Figure 2

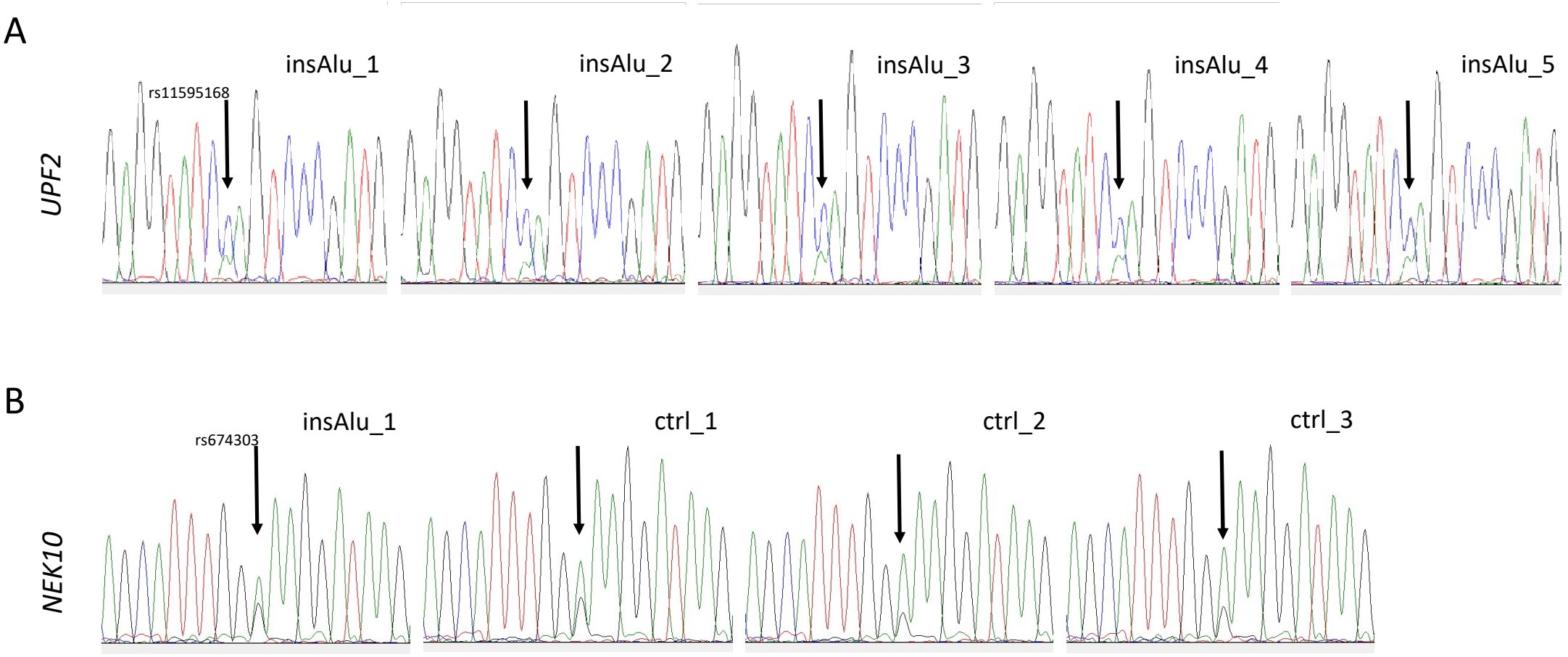
A
UPF2
rs11595168
insAlu_1
insAlu_2
insAlu_3
insAlu_4
insAlu_5
B
NEK10
rs674303
insAlu_1
ctrl_1
ctrl_2
ctrl_3

Figure 3

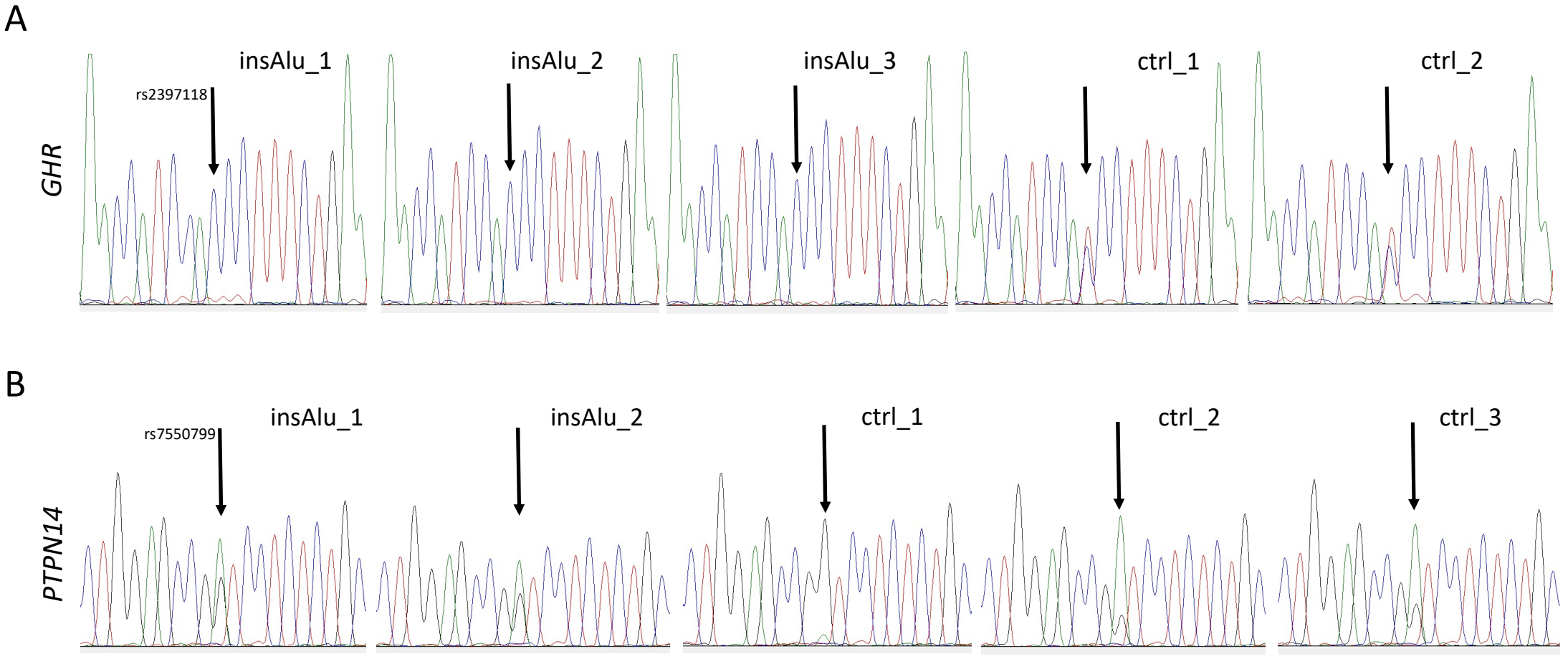
A
insAlu_1
insAlu_2
insAlu_3
ctrl_1
ctrl_2
rs2397118
GHR
B
insAlu_1
insAlu_2
ctrl_1
ctrl_2
ctrl_3
rs7550799
PTPN14

Figure 4

Figure 5